2014 American Control Conference (ACC)
June 4-6, 2014. Portland, Oregon, USA

Retrospective Cost Model Refinement for Aircraft Fault Signature Detection

Ming-Jui Yu, Kevin McDonough, Dennis S. Bernstein, and Ilya Kolmanovsky

***Abstract*— Retrospective cost model refinement is applied to on-board identification of a linearized aircraft model, and it is shown that with altitude and airspeed measurements, the aircraft stability derivatives can be estimated. These estimates are then compared to the nominal values at the same flight condition. The comparison between identified and nominal stability derivatives provides a fault signature. We also describe a methodology for updating the flight envelope based on identified stability derivatives.**

I. Introduction

Detection and identification of aircraft faults is essential for flight safety [1–3]. In this paper, we propose a two-step approach to detecting and identifying aircraft faults. In the first step, we accurately identify the current linear model and extract information on aircraft stability derivatives. In the second step, this information is compared to the nominal system and used to generate a fault signature.

This work is based on system identification from input-output data to construct empirical models. Some components of the system can be well-modeled while others are poorly modeled. The goal is to use input-output data to improve estimates of poorly modeled components. This problem is known as model updating, model correction, model calibration, and model refinement [4, 5].

The most common model-refinement problem is parameter estimation, where data are used to improve estimates of parameters in a model with a known structure. An unknown parameter may either be constant or time-varying in a pre-specified manner. The close relationship between parameter estimation and state estimation is evident from the widespread use of state-estimation techniques for parameter estimation. In particular, the extended Kalman filter can be used with a linearized model to propagate state and parameter estimates [6].

In this paper, we use retrospective cost model refinement (RCMR) [5, 7] to estimate parameters of an aircraft model with uncertain entries in the dynamics and input matrices. All of the examples are discrete time, as required by RCMR. To estimate all entries of the aircraft dynamics and input matrices, we develop a state augmentation technique for constructing the appropriate feedback structure.

Aircraft stability derivatives determine the static stability of an aircraft in steady flight. These are partial derivatives of forces and moments with respect to perturbations from the steady flight trim condition. The stability derivatives, once estimated, can provide information about the condition of the aircraft and the linear response of the aircraft to disturbances and control inputs.

In this paper we describe a process by which aircraft faults can be detected during flight by applying RCMR to identify a linear model followed by the inference of stability derivatives. The computations necessary for the model refinement and stability derivative estimation are inexpensive and thus can be performed on-board. However, to isolate faults, our method requires either supervisory logic or a searchable database, presumably built offline, to correlate the observed fault signature. We illustrate how the identified parameters of the linear model can be exploited to update the estimate of the flight envelope.

II. Identification Problem Formulation

Consider the MIMO discrete-time main system

$$x(k+1) = Ax(k) + Bu(k) + D_1 w(k), \tag{1}$$

$$y(k) = Cx(k), \tag{2}$$

$$y_0(k) = E_1 x(k) + v(k), \tag{3}$$

where $x(k) \in \mathbb{R}^n$, $y(k) \in \mathbb{R}^{l_y}$, $y_0(k) \in \mathbb{R}^{l_{y_0}}$, $u(k) \in \mathbb{R}^{l_u}$, $w(k) \in \mathbb{R}^{l_w}$, and $k \geq 0$. The main system (1)–(3) is interconnected with the unknown subsystem modeled by

$$u(k) = G_{\rm s}(q) y(k), \tag{4}$$

where q is the forward shift operator. The system (1)–(4) represents the true system. We assume that the excitation signal $w(k)$ is known. The measurement is y_0 and $v(k)$ denotes measurement noise.

Next, we assume a model of the main system of the form

$$\hat{x}(k+1) = \hat{A}\hat{x}(k) + \hat{B}\hat{u}(k) + \hat{D}_1 w(k), \tag{5}$$

$$\hat{y}(k) = \hat{C}\hat{x}(k), \tag{6}$$

$$\hat{y}_0(k) = \hat{E}_1 \hat{x}(k), \tag{7}$$

where $\hat{x}(k) \in \mathbb{R}^{\hat{n}}$, $\hat{y}(k) \in \mathbb{R}^{l_{\hat{y}}}$, $\hat{y}_0(k) \in \mathbb{R}^{l_{y_0}}$, $\hat{u}(k) \in \mathbb{R}^{l_{\hat{u}}}$. The model of the main system is interconnected with the subsystem model

$$\hat{u}(k) = \hat{G}_{\rm s}(q)\hat{y}(k). \tag{8}$$

The goal is to estimate a subsystem model, $\hat{G}_{\rm s}(q)$, by minimizing a cost function based on the performance variable

$$z(k) \stackrel{\triangle}{=} \hat{y}_0(k) - y_0(k) \in \mathbb{R}^{l_z}. \tag{9}$$

We estimate $\hat{G}_{\rm s}(q)$ by retrospectively reconstructing the signal $\hat{u}(k)$ that minimizes the performance variable cost

Ming-Jui Yu, Kevin McDonough, D. S. Bernstein, and Ilya Kolmanovsky are with the Department of Aerospace Engineering, University of Michigan, Ann Arbor, MI, USA. {mingray, kevinmcd, dsbaero, ilya}@umich.edu

978-1-4799-3271-9/$31.00 ©2014 AACC

at the current time step. The reconstruction of $\hat{u}(k)$ uses minimal modeling information about the true system (1)–(3), namely, a limited number of Markov parameters. We then use $\hat{u}(k)$ and $\hat{y}(k)$ to construct $\hat{G}_{\rm s}(q)$. Figure 1 illustrates the model-refinement architecture.

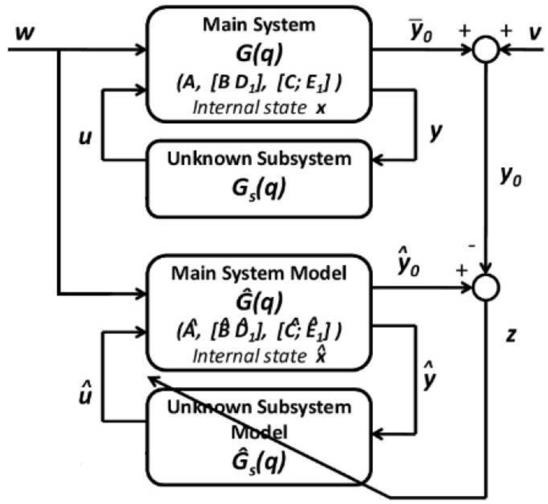

Fig. 1. Model refinement architecture.

The model refinement architecture can be used for parameter identification. Consider the case where the main system is not in feedback with an unknown subsystem, and the goal is to identify the matrix A. Let $\hat{G}_{\rm s}(q)$ be a static system of the form $\hat{u}(k) = \theta\hat{y}(k)$, where θ is based on z. The feedback system consisting of the main system model and the unknown subsystem model can be rewritten as

$$\hat{x}(k+1) = (\hat{A} + \hat{B}\theta\hat{C})\hat{x}(k) + \hat{D}_1 w(k), \tag{10}$$

$$\hat{y}_0(k) = \hat{E}_1\hat{x}(k). \tag{11}$$

Assuming that we have knowledge of D_1 and E_1, we let $\hat{D}_1 = D_1$ and $\hat{E}_1 = E_1$ and we postulate that $A = \hat{A} + \Delta A$. To identify entries of A, we choose $\hat{B}$ and $\hat{C}$ and update θ such that $\hat{B}\theta\hat{C}$ converges to ΔA. To identify all parameters in A, we set $\hat{B}$ and $\hat{C}$ equal to the identity and update $\theta \in \mathbb{R}^{n\times n}$.

III. Retrospective Cost Model Refinement

We apply retrospective cost optimization to update θ. In the present paper, we provide only a brief overview of RCMR. A detailed formulation is given in [5, 7].

We begin by defining Markov parameters of the main system model $\hat{G}(q)$. For $i \geq 1$, let

$$H_i \stackrel{\triangle}{=} \hat{E}_1\hat{A}^{i-1}\hat{B}. \tag{12}$$

Therefore, $H_1 = \hat{E}_1\hat{B}$ and $H_2 = \hat{E}_1\hat{A}\hat{B}$. Let r be a positive integer. Then, for all $k \geq r$,

$$z(k) = \hat{E}_1\hat{A}^r\hat{x}(k-r) + \sum_{i=1}^{r}\hat{E}_1\hat{A}^{i-1}\hat{D}_1 w(k-i) - y_0(k) + \bar{\mathcal{H}}\bar{U}(k-1), \tag{13}$$

where $\bar{\mathcal{H}} \stackrel{\triangle}{=} \left[\begin{array}{ccc} H_1 & \cdots & H_r \end{array}\right] \in \mathbb{R}^{l_z\times rl_{\hat{u}}}$, and

$$\bar{U}(k-1) \stackrel{\triangle}{=} \left[\begin{array}{ccc} \hat{u}^{\rm T}(k-1) & \cdots & \hat{u}^{\rm T}(k-r) \end{array}\right]^{\rm T}.$$

Next, we rearrange the columns of $\bar{\mathcal{H}}$ and the components of $\bar{U}(k-1)$ and partition the resulting matrix and vector so that

$$\bar{\mathcal{H}}\bar{U}(k-1) = \mathcal{H}'U'(k-1) + \mathcal{H}U(k-1), \tag{14}$$

where $\mathcal{H}' \in \mathbb{R}^{l_z\times(rl_{\hat{u}}-l_U)}$, $\mathcal{H} \in \mathbb{R}^{l_z\times l_U}$, $U'(k-1) \in \mathbb{R}^{rl_{\hat{u}}-l_U}$, and $U(k-1) \in \mathbb{R}^{l_U}$. Then, we can rewrite (13) as

$$z(k) = \mathcal{S}(k) + \mathcal{H}U(k-1), \tag{15}$$

where

$$\mathcal{S}(k) \stackrel{\triangle}{=} \hat{E}_1\hat{A}^r\hat{x}(k-r) + \sum_{i=1}^{r}\hat{E}_1\hat{A}^{i-1}\hat{D}_1 w(k-i) - y_0(k) + \mathcal{H}'U'(k-1). \tag{16}$$

Then, if we define

$$Z(k) \stackrel{\triangle}{=} \left[\begin{array}{ccc} z^{\rm T}(k-k_1) & \cdots & z^{\rm T}(k-k_s) \end{array}\right]^{\rm T} \in \mathbb{R}^{sl_z} \tag{17}$$

and $\tilde{\mathcal{S}}(k) \stackrel{\triangle}{=} \left[\begin{array}{c} \mathcal{S}^{\rm T}(k-k_1)\cdots\mathcal{S}^{\rm T}(k-k_s) \end{array}\right]^{\rm T} \in \mathbb{R}^{sl_z}$, we can write

$$Z(k) = \tilde{\mathcal{S}}(k) + \tilde{\mathcal{H}}\tilde{U}(k-1), \tag{18}$$

Next, we define the *retrospective performance*

$$\hat{z}(k) \stackrel{\triangle}{=} \mathcal{S}(k) + \mathcal{H}U^*(k-1), \tag{19}$$

where the actual past subsystem outputs $U(k-1)$ in (18) are replaced by the surrogate subsystem outputs $U^*(k-1)$. The *extended retrospective performance* for (19), which is defined as

$$\hat{Z}(k) \stackrel{\triangle}{=} \left[\begin{array}{ccc} \hat{z}^{\rm T}(k-k_1) & \cdots & \hat{z}^{\rm T}(k-k_s) \end{array}\right]^{\rm T} \in \mathbb{R}^{sl_z}, \tag{20}$$

is given by

$$\hat{Z}(k) = \tilde{\mathcal{S}}(k) + \tilde{\mathcal{H}}\tilde{U}^*(k-1), \tag{21}$$

where the components of $\tilde{U}^*(k-1) \in \mathbb{R}^{l_{\tilde{U}}}$ are components of $U_1^*(k-k_1-1), \ldots, U_s^*(k-k_s-1)$ ordered in the same way as the components of $\tilde{U}(k-1)$. Subtracting (18) from (21) yields

$$\hat{Z}(k) = Z(k) - \tilde{\mathcal{H}}\tilde{U}(k-1) + \tilde{\mathcal{H}}\tilde{U}^*(k-1). \tag{22}$$

A. Cost Function Optimization with Adaptive Regularization

We consider the regularized cost

$$\bar{J}(\tilde{U}^*(k-1), k) \stackrel{\triangle}{=} \hat{Z}^{\rm T}(k)R(k)\hat{Z}(k) + \eta(k)\tilde{U}^{*\rm T}(k-1)\tilde{U}^*(k-1), \tag{23}$$

where $\eta(k) = \bar{\eta}z^{\rm T}(k)z(k)$ and $\bar{\eta} \geq 0$. Substituting (22) into (23) yields

$$\bar{J}(\tilde{U}^*(k-1), k) = \tilde{U}^*(k-1)^{\rm T}\mathcal{A}(k)\tilde{U}^*(k-1) + \mathcal{B}(k)\tilde{U}^*(k-1) + \mathcal{C}(k), \tag{24}$$

where

$$\mathcal{A}(k) \stackrel{\triangle}{=} \tilde{\mathcal{H}}^{\rm T}R(k)\tilde{\mathcal{H}} + \eta(k)I_{l_{\tilde{U}}}, \tag{25}$$

$$\mathcal{B}(k) \stackrel{\triangle}{=} 2\tilde{\mathcal{H}}^{\rm T}R(k)[Z(k) - \tilde{\mathcal{H}}\tilde{U}(k-1)], \tag{26}$$

$$\mathcal{C}(k) \triangleq Z^{\mathrm{T}}(k)R(k)Z(k) - 2Z^{\mathrm{T}}(k)R(k)\tilde{\mathcal{H}}\tilde{U}(k-1) + \tilde{U}^{\mathrm{T}}(k-1)\tilde{\mathcal{H}}^{\mathrm{T}}R(k)\tilde{\mathcal{H}}\tilde{U}(k-1). \quad (27)$$

If either $\tilde{\mathcal{H}}$ has full column rank or $\eta(k) > 0$, then $\mathcal{A}(k)$ is positive definite. In this case, $\bar{J}(\tilde{U}^*(k-1), k)$ has the unique global minimizer

$$\tilde{U}^*(k-1) = -\frac{1}{2}\mathcal{A}^{-1}(k)\mathcal{B}(k). \quad (28)$$

B. Subsystem Modeling

The subsystem output $\hat{u}(k)$ is given by the exactly proper time-series model of order n_{c} given by

$$\hat{u}(k)=\sum_{i=1}^{n_{\mathrm{c}}} M_i(k)\hat{u}(k-i)+\sum_{i=0}^{n_{\mathrm{c}}} N_i(k)\hat{y}(k-i)+\sum_{i=0}^{n_{\mathrm{c}}} O_i(k)w(k-i), \quad (29)$$

where, for all $i = 1, \ldots, n_{\mathrm{c}}$, $M_i(k) \in \mathbb{R}^{l_{\hat{u}} \times l_{\hat{u}}}$, $N_i(k) \in \mathbb{R}^{l_{\hat{u}} \times l_{\hat{y}}}$ and $O_i(k) \in \mathbb{R}^{l_{\hat{u}} \times l_w}$.

If $n_c = 0$, then

$$\hat{u}(k) = N_0(k)\hat{y}(k) \triangleq \theta(k)\phi(k-1). \quad (30)$$

C. Recursive Least Squares Update

Let $d > 0$ such that $\tilde{U}^*(k-1)$ contains $u^*(k-d)$, and define the retrospective cost function

$$J_{\mathrm{R}}(\theta(k)) \triangleq \sum_{i=1}^{k} \lambda^{k-i}||u^{*\mathrm{T}}(k-d) - \phi^{\mathrm{T}}(k-d-1)\theta^{\mathrm{T}}(k)||^2 + \lambda^k(\theta(k) - \theta(0))P^{-1}(0)(\theta(k) - \theta(0))^{\mathrm{T}},$$

where $\phi(k-d)$ is given by (30) with delay, $\|\cdot\|$ is the Euclidean norm, and $\lambda(k) \in (0, 1]$ is the forgetting factor. Minimizing the cumulative cost function yields the parameter update

$$\theta^{\mathrm{T}}(k) = \theta^{\mathrm{T}}(k-1) + P(k-1)\phi(k-d-1) \cdot [\phi^{\mathrm{T}}(k-d)P(k-1)\phi(k-d-1) + \lambda(k)]^{-1} \cdot (u^*(k-d) - \phi^{\mathrm{T}}(k-d-1)\theta^{\mathrm{T}}(k-1)). \quad (31)$$

The error covariance is updated by

$$P(k) =\lambda^{-1}(k)P(k-1) - \lambda^{-1}(k)P(k-1)\phi(k-d-1) \cdot [\phi^{\mathrm{T}}(k-d-1)P(k-1)\phi(k-d) + \lambda(k)]^{-1} \cdot \phi^{\mathrm{T}}(k-d-1)P(k-1). \quad (32)$$

We initialize the error covariance matrix as $P(0) = \beta I$, where $\beta > 0$.

IV. Parameter Estimation Using State Augmentation

The method outlined in section II can be used to identify entries of the aircraft dynamics matrix A. However, degradations may also occur in the actuation sensitivity of an aircraft, which corresponds to changes in D_1. We now formulate a method to concurrently identify entries in both A and D_1 of the linearized aircraft model.

Consider the known exogenous signal $w_a(k)$ given by

$$w_a(k+1) = w(k), \quad (33)$$

and define

$$X(k) \triangleq \begin{bmatrix} x(k) \\ w_a(k) \end{bmatrix}. \quad (34)$$

The main system can then be rewritten with the augmented state $X(k)$ as

$$X(k+1) = \begin{bmatrix} A & D_1 \\ 0 & 0 \end{bmatrix} X(k) + \begin{bmatrix} B \\ 0 \end{bmatrix} u(k) + \begin{bmatrix} 0 \\ I \end{bmatrix} w(k), \quad (35)$$

$$y(k) = \begin{bmatrix} C & 0 \end{bmatrix} X(k), \quad (36)$$

$$y_0(k) = \begin{bmatrix} E_1 & 0 \end{bmatrix} X(k) + v(k) \quad (37)$$

This augmented system includes the exogenous signal as a state and thus incorporates D_1 in the system dynamics allowing for simultaneous identification of A and D_1. The main system model can be written in a similar augmented form by defining

$$\hat{X}(k) \triangleq \begin{bmatrix} \hat{x}(k) \\ w_a(k) \end{bmatrix} \quad (38)$$

By applying RCMR to the augmented main system, both A and D_1 can be estimated.

V. Fault Signatures

We define an aircraft fault signature as a vector with components that are the percent difference between estimated values, X_{est}, and nominal values, X_{nom}, of stability derivatives.

To isolate faults, either supervisory logic is necessary to interpret the fault signatures or a searchable database that contains fault signatures and their corresponding faults.

A. Finding and Using Fault Signatures

To find a fault signature, we solve the equations used to describe the entries of the A and B of the linear systems for the stability derivatives of the identified system and compare them to the nominal stability derivatives for the same flight condition.

The equations that are used to calculate the entries of A and B can be found in [8]. As an example, the (1,3) entry of A for the longitudinal dynamics, X_q, is

$$X_q = \frac{p_d S\bar{c}}{2mU_0} C_{\mathrm{D}q}, \quad (39)$$

where p_d is the dynamic pressure, S is the wing surface area, $\bar{c}$ is the wing mean chord, m is the aircraft mass, U_0 is the aircraft airspeed for this flight condition, and C_{Dq} is the stability derivative of drag force with respect to perturbations in pitch rate. The estimate of $C_{\mathrm{D}q}$, $\hat{C}_{\mathrm{D}q}$, is

$$\hat{C}_{\mathrm{D}q} = \hat{X}_q \frac{2mU_0}{p_d S\bar{c}}. \quad (40)$$

The system of equations generated for all entries of A and B, a similar equation to (40) for each entry, can be written succinctly as a function of a set of aircraft parameters, p_a, the identified linear system, $\hat{\Sigma}$, and the stability derivatives we seek to find, C_x, as $f(p_a, \hat{\Sigma}, C_x)$ and we seek to solve for the values of C_x such that

$$f(p_a, \hat{\Sigma}, C_x) = 0. \tag{41}$$

Different percent differences may correspond to different types of faults. For example, if every component of the fault signature has the same value, then an error is likely occurring in sensor measurements related to dynamic pressure. However, if the aircraft fault signature is a vector of zeros, this indicates that there is no fault and the aircraft is functioning normally.

Because the identification is performed on a discrete system, the identified system is transformed to continuous time in order to perform the fault signature analysis.

VI. Aircraft Example

An aircraft icing example is now presented where the lift and drag forces are multiplied by constant factors, as in [3]. Specifically, the lift force is reduced by 50% and the drag force is increased by 50%.

In order to represent the changes in the drag and lift forces in the linear models, we take advantage of the fact that the coefficient of lift and the coefficient of drag can be approximated as functions of stability derivatives. The coefficient of lift is

$$C_{\rm L} \approx C_{\rm L0} + \frac{1}{U_0} C_{{\rm L}u} u + \frac{\bar{c}}{2U_0} C_{{\rm L}q} q + C_{{\rm L}\alpha} \delta\alpha + C_{{\rm L}\delta e} \delta e, \tag{42}$$

and the coefficient of drag is

$$C_{\rm D} \approx C_{\rm D0} + \frac{1}{U_0} C_{{\rm D}u} u + \frac{\bar{c}}{2U_0} C_{{\rm D}q} q + C_{{\rm D}\alpha} \delta\alpha + C_{{\rm D}\delta e} \delta e. \tag{43}$$

In (42) and (43), u, q, $\delta\alpha$, and δe are, respectively, the deviations of airspeed, pitch rate, angle of attack, and elevator deflection from the trim condition. Therefore, to represent changes in lift and drag within the linear models, we multiply the stability derivatives associated with lift and drag by corresponding factors.

The nominal aircraft dynamics based on the Generic Transport Model (GTM), [9, 10], linearization at the nominal condition of $h = 1000$ ft, $U_0 = 550$ fps, and $\alpha = 5$ deg are given by

$$\dot{x} = A_{\rm nom} x + B_{\rm nom} u, \tag{44}$$

where

$$A_{\rm nom} = \begin{bmatrix} -0.0147 & 2.1539 & -1.9270 & -32.2000 \\ -0.0005 & -1.0543 & 0.9611 & 0 \\ 0.0019 & -2.7969 & -0.8428 & 0 \\ 0 & 0 & 1 & 0 \end{bmatrix},$$

$$B_{\rm nom} = \begin{bmatrix} 5.8737 & 3.3333 \\ -0.0923 & 0 \\ -3.7674 & 0 \\ 0 & 0 \end{bmatrix}, \tag{45}$$

with $x = [u\ \alpha\ q\ \theta]^{\rm T}$ and $u = [\delta e\ \delta T]^{\rm T}$.

Discretizing (45) using a zero-order hold with $T_s = 0.5s$ yields

$$A = \begin{bmatrix} 0.9910 & 1.7253 & -2.4488 & -16.0382 \\ 0 & 0.3960 & 0.2669 & 0.0006 \\ 0.0008 & -0.7758 & 0.4541 & -0.0070 \\ 0.0002 & -0.2433 & 0.3693 & 0.9988 \end{bmatrix},$$

$$D_1 = \begin{bmatrix} 4.2298 & 1.6603 \\ -0.3476 & -0.0001 \\ -1.3674 & 0.0007 \\ -0.3871 & 0.0001 \end{bmatrix}.$$

At the beginning of the simulation, the coefficient of lift of the aircraft is decreased by 50% while the coefficient of drag is increased by 50%. This produces changes in A and D_1 given by

$$\Delta A = \begin{bmatrix} -0.0037 & -25.6453 & -5.6189 & 0.0270 \\ 0.0001 & 0.1336 & 0.0426 & -0.0008 \\ -0.0001 & -0.1180 & -0.0240 & 0.0004 \\ 0 & -0.0229 & -0.0035 & 0 \end{bmatrix},$$

$$\Delta D_1 = \begin{bmatrix} 4.3406 & -0.0028 \\ -0.0377 & 0.0001 \\ 0.0154 & 0 \\ 0.0018 & 0 \end{bmatrix}.$$

We choose δe and δT to be zero-mean white Gaussian noises with variances 10^{-8} and 10^{-3}. We also assume full state and actuation measurements, meaning that $E_1 = I_4$. For identification, we choose $\hat{C} = I_6$ and $\hat{B} = \begin{bmatrix} I_4 & 0 \end{bmatrix}^{\rm T}$, which means that $\theta(k) = \begin{bmatrix} \Delta\hat{A} & \Delta\hat{D}_1 \end{bmatrix}$.

The tuning parameters chosen for this example are $P(0) = 1000$, $\lambda = 0.995$, $\eta = 0$, and $\tilde{\mathcal{H}} = H_1$. Figures 2, 3, and 4 show the identification of each parameter in the matrices A and D_1. Figure 5 shows $z = y_0 - \hat{y}_0$ over time. The importance of this is to show the convergence of z to 0 over time because this corresponds to the minimization of the performance cost function. All identified parameters converge to the correct values within 5000 time steps except for $\Delta D_{1_{11}}$, which converges in 8000 time steps.

Figure 6 shows percent differences in $2C_{\rm D0} + C_{{\rm D}u}$, $C_{\rm L0} - C_{{\rm D}\alpha}$, $C_{{\rm D}q}$, $C_{L0} - C_{{\rm L}u}$, $C_{{\rm L}\alpha} + C_{\rm D0}$, $C_{{\rm L}q}$, $2C_{\rm m0} + C_{{\rm m}u}$, $C_{{\rm m}\alpha}$, $C_{{\rm m}q}$, $C_{{\rm D}\delta e}$, $C_{{\rm L}\delta e}$, $C_{{\rm m}\delta e}$, and $C_{{\rm D}\delta th}$, respectively labeled components 1 through 12 in Figure 6, based on the identified linear model. As can be seen, components 4 and 5, which are entirely associated with lift, are roughly half the nominal value and components 1 and 3, which are associated with drag, are roughly 1.5 times their nominal level. Entry 2 is substantially more negative than the nominal value. This is consistent with a reduction in $C_{\rm L0}$ and an increase in $C_{\rm D0}$ because nominally $C_{\rm L0}$ and $C_{\rm D0}$ are approximately the same magnitude. Because $C_{{\rm L}\alpha}$ is 100 times larger than $C_{\rm D0}$, relatively large increases in drag would not impact this term greatly and thus the changes in lift dominate the entry.

A. Estimating $\hat{\alpha}_{max}$ from Identified Stability Derivatives

When an aircraft fault occurs, it is necessary to determine changes in boundaries of the nominal flight envelope. We

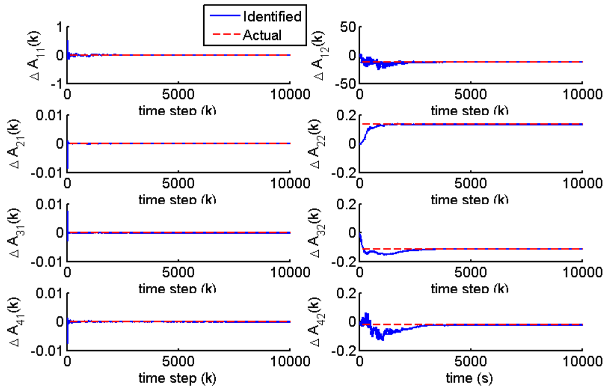

Fig. 2. Identification of $A(1\text{-}4{,}1\text{-}2)$.

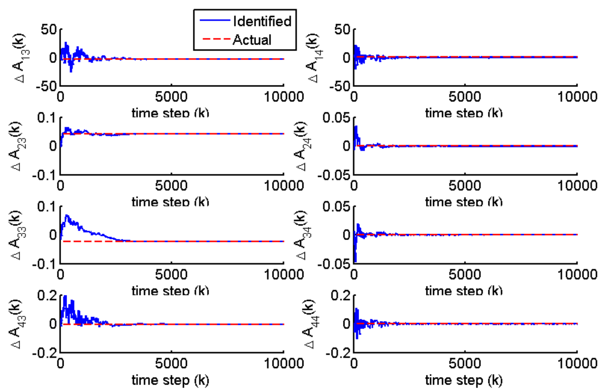

Fig. 3. Identification of $A(1\text{-}4{,}3\text{-}4)$.

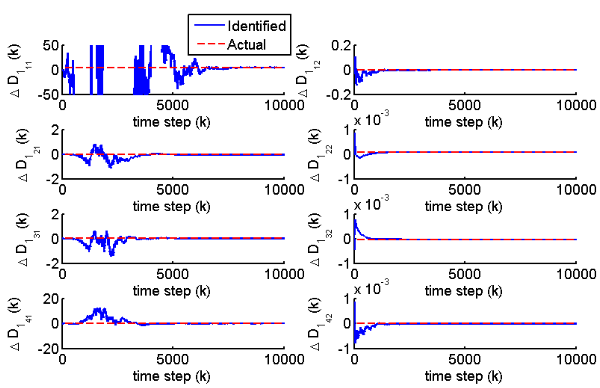

Fig. 4. Identification of the matrix D_1.

now present a method for estimating $\hat{\alpha}_{\max}$, the maximum achievable angle of attack without a loss of lift, after a fault has occurred.

Once a linear system is identified and stability derivatives are estimated, we use (42) and knowledge of the nominal value of the maximum coefficient of lift, C_{Lmax}, to estimate the value of the maximum coefficient of lift for the post fault system, $\hat{C}_{\mathrm{Lmax}}$, and a maximum deviation from the current angle of attack, $\delta\alpha_{\max}$.

We do this first by assuming C_{Lmax} is similarly affected

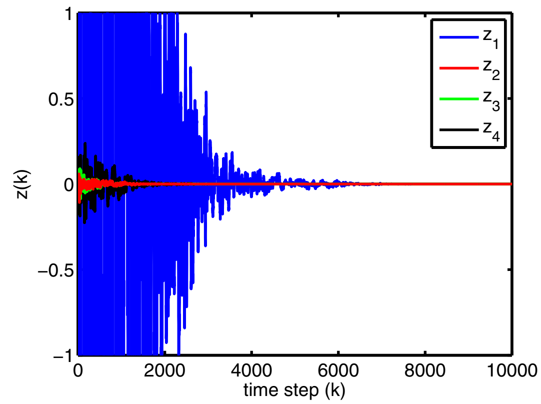

Fig. 5. Performance $z(k)$ is the difference between the states of the aircraft and the nominal aircraft model. Parameter estimates are found as $z(k)$ converges to zero.

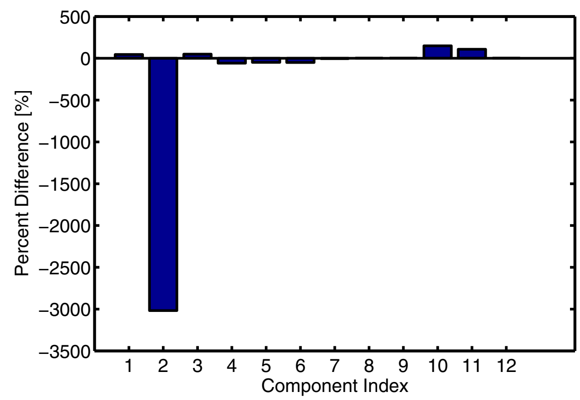

Fig. 6. The fault signature for the Aircraft Icing problem

as C_{L} in (42), i.e.,

$$\hat{C}_{\mathrm{Lmax}} = C_{\mathrm{Lmax}}(1 + \frac{\mathrm{PD}_{C_{\mathrm{L}}}}{100}), \tag{46}$$

where $\mathrm{PD}_{C_{\mathrm{L}}}$ is the average percent difference between the estimated values of stability derivatives associated with lift and their nominal value and C_{Lmax} is the nominal value of the maximum coefficient of lift. To generate the estimate of $\delta\alpha_{\max}$, we employ (42) and define a constant $\bar{C}_{\mathrm{L0}}$ to be the sum of all entries of (42) that do not depend on angle of attack such that

$$\delta\alpha_{\max} \approx \frac{\hat{C}_{\mathrm{Lmax}} - \bar{C}_{\mathrm{L0}}}{\hat{C}_{\mathrm{L}\alpha}}, \tag{47}$$

where $\hat{C}_{\mathrm{L}\alpha}$ is the estimated value of $C_{\mathrm{L}\alpha}$ post fault. It then follows that

$$\hat{\alpha}_{\max} = \alpha_0 + \delta\alpha_{\max}, \tag{48}$$

where α_0 is the trim value of the angle of attack post fault.

From (47) and (48), it is clear that if a fault such as the icing example presented earlier is observed, then $\alpha_{\max}$ remains unchanged. However, if the stability derivatives related to lift are not uniformly altered, the estimate of $\alpha_{\max}$ changes similarly. As an example, for the nominal system, assume $C_{\text{Lmax}} = 1.3691$, of C_{L0} is 0.5113, and of $C_{\text{L}\alpha}$ is 5.1891. Next, we assume that the fault signature of an identified system for the same flight condition as above indicates that C_{L0} is halved but $C_{L\alpha}$ is unchanged. We assume that C_{Lmax} is affected similarly to C_{L0} and thus $\hat{C}_{\text{L0}} = 0.2557$ and $\hat{C}_{\text{Lmax}} = 0.6845$. If the only deviation from the trim condition is in α, then $\bar{C}_{L0} = \hat{C}_{L0}$. Therefore, from (47), $\delta\alpha_{\text{max}} = 4.74$ deg, which results in $\hat{\alpha}_{\text{max}} = 9.74$ deg. This is in contrast to the nominal value of the critical angle of attack of $\alpha_{\text{max}} = 14.48$ deg.

B. Estimating the Steady Flight Envelope Boundary

The stability derivative estimate can be used to update the boundaries of the static flight envelope, which characterizes the set of aircraft states in which the aircraft can fly in steady-state. The longitudinal static flight envelope is described by the constraints

$$V \geq \sqrt{\frac{2W}{\rho S C_{\text{Lmax}}}}, \tag{49}$$

$$W\gamma + 1/2\rho V^2 S C_{D0} + \frac{2KW^2}{\rho S V^2 \cos^2\phi} \leq \left(\frac{\rho}{\rho_s}\right)^m T^s_{\text{max}}, \tag{50}$$

where, for the aircraft we consider, $W = 193200$ lb is the aircraft weight, γ is the flight path angle, ϕ is the roll angle, $K = \frac{1}{\pi A R e_0} = 0.531$, where AR is the aircraft aspect ratio, e_0 is the Oswald efficiency factor, $\rho_s = 0.0024\ \frac{\text{slug}}{\text{ft}^3}$ is the air pressure at sea level, and $T^s_{\text{max}} = 80000$ lbs is the maximum engine thrust at sea level. These constraints are the airspeed stall constraint, (49), and the maximum thrust constraint, (50), and are used to determine the boundary and interior of areas shown in Figure 7.

The pre-fault value of C_{Lmax} is the same as above, and the pre-fault value of the zero lift drag coefficient is $C_{\text{D0}} = 0.1$. Applying the observed post-fault changes from above, the values of the estimated parameters are $\hat{C}_{\text{Lmax}} = 0.6845$ and $\hat{C}_{\text{D0}} = 0.15$. Figure 7 shows that these changes can be used to update estimates of the static flight envelope boundary. As expected, an increase in drag and decrease in lift results in a smaller flight envelope. For these results, it is assumed $\gamma = \phi = 0$ deg.

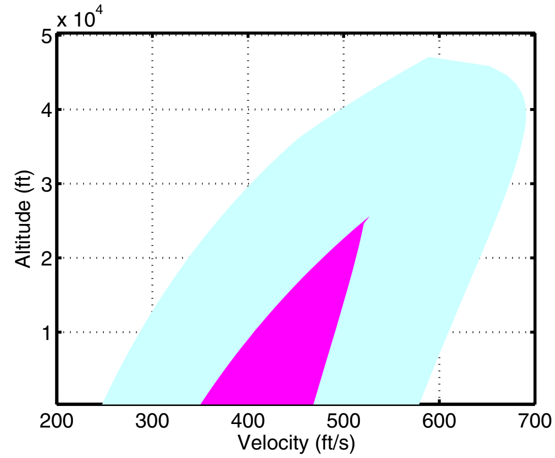

Fig. 7. The nominal longitudinal static flight envelope (light blue) compared with an estimate of the longitudinal static flight envelope for the identified system (pink).

VII. Conclusions

In this paper, it has been shown that retrospective cost model refinement can be used to identify a linear aircraft model after an aircraft fault has occurred. This information may then be used to infer stability derivatives and generate fault signature vectors to facilitate fault detection. Stability derivatives inferred with this approach can also be used for flight envelope estimation following on-board failures.

Acknowledgements

This research is supported by NASA under contract number NNX12AM54A. The authors would like to thank Ella Atkins and Sweewarman Balachandran for their help and support.

References

[1] H. G. Kwatny, J.-E. T. Dongmo, R. C. Allen, B.-C. Chang, and G. Bajpai, "Loss-of-control: Perspectives on flight dynamics and control of impaired aircraft," in *AIAA Conference on Guidance, Navigation, and Control, Toronto*, 2010.

[2] T. Lombaerts, Q. Chu, J. A. Mulder, and D. Joosten, "Flight control reconfiguration based on a modular approach," in *Fault Detection, Supervision and Safety of Technical Processes*, 2009, pp. 259–264.

[3] M. B. Bragg, T. Basar, W. R. Perkins, M. S. Selig, P. G. Voulgaris, J. W. Melody, and N. B. Sarter, "Smart icing systems for aircraft icing safety," *AIAA Paper*, vol. 813, 2002.

[4] H. Palanthandalam-Madapusi, E. L. Renk, and D. S. Bernstein, "Data-based model refinement for linear and Hammerstein systems using subspace identification and adaptive disturbance rejection," in *Proc. Conf. Contr. Appl.*, Toronto, Canada, August 2005, pp. 1630–1635.

[5] A. M. D'Amato, A. R. Wu, K. S. Mitchell, S. L. Kukreja, and D. S. Bernstein, "Damage localization for structural health monitoring using retrospective cost model refinement," in *Proc. AIAA SDM Conf.*, Orlando, FL, April 2010, aIAA-2010-2628.

[6] L. Ljung, "Asymptotic behavior of the extended kalman filter as a parameter estimator for linear systems," *IEEE Trans. Autom. Control*, vol. 24, pp. 36–50, 1979.

[7] A. M. D'Amato and D. S. Bernstein, "Linear fractional transformation identification using retrospective cost optimization," in *Proc. SYSID*, Saint-Malo, France, July 2009, pp. 450–455.

[8] B. L. Stevens and F. L. Lewis, *Aircraft control and simulation*, ser. Wiley-Interscience. New York, Chichester, Brisbane: J. Wiley and sons, 1992.

[9] I. Ix and I. Iz, "Practical application of a subscale transport aircraft for flight research in control upset and failure conditions," 2008.

[10] N. T. Nguyen, K. S. Krishnakumar, J. T. Kaneshige, and P. P. Nespeca, "Flight dynamics and hybrid adaptive control of damaged aircraft," *Journal of guidance, control, and dynamics*, vol. 31, no. 3, pp. 751–764, 2008.